A unified approach to engine cylinder pressure reconstruction using time-delay neural networks with crank kinematics or block vibration measurements

Article (Accepted Version)

A UNIFIED APPROACH TO ENGINE CYLINDER PRESSURE RECONSTRUCTION USING TIME-DELAY NEURAL NETWORKS WITH CRANK KINEMATICS OR BLOCK VIBRATION MEASUREMENTS

by

S. Trimby, J.F. Dunne*, C. Bennett, and D. Richardson †

Department of Engineering and Design
School of Engineering and Informatics
University of Sussex, Falmer, Brighton, BN1 9QT, UK.
* Corresponding author: E-mail: j.f.dunne@sussex.ac.uk

† Powertrain Research & Technology, Jaguar Land Rover
Viscount 2 (W11/8 Unit C2), Millburn Hill Road,
Cannon Park, Coventry, CV4 7HS

ABSTRACT

Closed-loop combustion control (CLCC) in gasoline engines can improve efficiency, calibration effort, and performance using different fuels. Knowledge of in-cylinder pressures is a key requirement for CLCC. Adaptive cylinder pressure reconstruction offers a realistic alternative to direct sensing, which is otherwise necessary as legislation requires continued reductions in CO_2 and exhaust emissions. Direct sensing however is expensive and may not prove adequately robust. A new approach is developed for in-cylinder pressure reconstruction on gasoline engines. The approach uses Time-Delay feed-forward Artificial Neural Networks trained with the standard Levenberg-Marquardt algorithm. The same approach can be applied to reconstruction via measured crank kinematics obtained from a shaft encoder, or measured engine cylinder block vibrations obtained from a production knock sensor. The basis of the procedure is initially justified by examination of the information content within measured data, which is considered to be equally important as the network architecture and training methodology. Key hypotheses are constructed and tested using data taken from a 3-cylinder (DISI) engine to reveal the influence of the data information content on reconstruction potential. The findings of these hypotheses tests are then used to develop the methodology. The approach is tested by reconstructing cylinder pressure across a wide range of steady-state engine operation using both measured crank kinematics and block accelerations. The results obtained show a very marked improvement over previously published reconstruction accuracy for both crank kinematics and cylinder block vibration based reconstruction using measurements obtained from a multi-cylinder engine. The paper shows that by careful processing of measured engine data, a standard neural network architecture and a standard training algorithm can be used to very accurately reconstruct engine cylinder pressure with high levels of robustness and efficiency.

27 main-section pages (double spaced) 23 references Figures 1 – 13 No appendices

1. INTRODUCTION

Knowledge of in-cylinder pressure is important for IC engine closed-loop combustion control, particularly for increasing thermal efficiency. Closed-loop combustion control can reduce both tailpipe and NVH emissions [1] and can improve performance following cold start [2]. A pressure trace can be used to optimise engine performance, efficiency, and emissions. But it also contains combustion parameter information such as peak pressure, rates-of-change of pressure, IMEP, and ignition timing, useful for knock and misfire detection, cylinder balancing, reduction of cycle-by-cycle variability, control of NVH, and after-treatment. Knock and air fuel ratio control, are achieved using knock and lambda sensor signals. However for combustion control, sensing of cylinder pressure is needed for combustion monitoring. Pressure sensors are available for test engines but are too expensive for production engines. They also suffer from durability and packaging issues. The use of torque sensors [3] can be viewed as a direct route to cylinder pressure reconstruction but they are also expensive and some form of dynamic model is needed.

Attempts have been made to use indirect sensing methods to reconstruct cylinder pressure in real time by processing signals from existing sensors already fitted to the engine. To do this, an inverse nonlinear dynamic model is needed which identifies the source of excitation (i.e. cylinder pressure) from the measured response, such as crank kinematics, block or head vibrations. Unfortunately two problems arise with physical models. First, calibration is difficult owing to singular behavior at TDC, precisely where high pressure information is dominant. And second, no two engines are identical owing to variability in materials, manufacture, or assembly. This means that a model calibrated on one engine may not work well on a nominally identical engine. Some form of adaptive capability is needed. The focus of this paper is on the first of these two problems, namely finding an accurate indirect reconstruction methodology using artificial neural networks.

Crankshaft kinematic-based reconstruction has been attempted in [4] using crank speed fluctuations. Similar approaches have been used in [5-6] to produce similar accuracy, and in [7], machine learning was used via radial basis function (RBF) networks. Work in [8-9] used non-parametric models to reconstruct cylinder pressure, which were tested on 2.5 L 4-cylinder diesel engine. An average peak pressure error of 5% and a location of peak pressure error of ± 2°CA was obtained. An alternative approach was adopted in [10] using engine speed fluctuations and a single pressure sensor on a multi-cylinder engine. Reconstruction used a combination of torque and pressure on a 4-cylinder SI engine. Peak pressure errors were obtained in the range of 6%, with the position of peak pressure error at 3°CA. A NARX neural network architecture was used in [11] trained on crank kinematics. Two fully-recurrent training algorithms were validated on a 1.12 L DISI engine fitted with spark-plug mounted pressure sensors on all cylinders, and a shaft encoder. Training was achieved via the Back-Propagation-Through-Time (BPTT) algorithm, and the Extended Kalman Filter (EKF). Both were extremely slow but reconstruction accuracy was promising giving peak pressure errors below 2%. However, in localised regions, errors increased to 25%, and in some cases became unstable. Interestingly, the EKF has been applied directly to an empirical, zero-dimensional, cylinder pressure reconstruction model in [12]. Work continued using recurrent neural networks in [13] where reconstruction was attempted on an SI engine using a two-zone model to generate additional data. Peak pressure predictions were consistently around 10% error. Crank speed fluctuations were studied in [14] to estimate the cylinder pressure trace, peak pressure, position of peak pressure, and ignition delay. Two model-based approaches were adopted i.e.: a complex fully-dynamic model that included crank flexibility, and a simpler model which included inertia torque, but omitted crank flexibility and friction. Both approaches were tested on 2.5L 4-cylinder VM Motori engine, fitted with a pressure sensor and shaft encoder.

Although results using both models were poor, they highlight important limitations for model-based reconstruction, specifically the effect of crankshaft flexibility and friction. Combustion parameters were obtained in [15] differently from those discussed earlier i.e. by directly obtaining the magnitude of peak pressure and the angular location of peak pressure. A neural network was tested on a boosted single-cylinder gasoline research engine fitted with a pressure sensor and a high resolution encoder to obtain instantaneous crank kinematics with 0.1°CA crank angle precision. A Multi-Layer-Perceptron (MLP) network fed with crank speed and acceleration, and two outputs (peak pressure, and location of peak pressure) was trained using (feed-forward) Bayesian regularisation. The lowest relative error for peak pressure was 4% reaching as high as 20% but the error on the location of peak pressure was better, between 4.8% and 9.1%. For crank kinematic-based prediction these results show that there are no significant advantages of using neural networks to directly reconstruct combustion parameters rather than obtaining the entire pressure trace.

Block-Acceleration-based reconstruction was first attempted in [16] using an ‘expectation–maximization’ algorithm to estimate cylinder pressure. This was tested on a 1.8 L 4-cylinder, turbocharged SI engine. Spark-plug mounted pressure sensors were used on all cylinders, plus four accelerometers mounted just below the cylinder head. Results show relatively good reconstruction with a correlation coefficient of 0.9. However, when expanding to 1000 cycles, the correlation coefficient for generalised results drop significantly to 0.68. Work in [17] combined engine block-vibration and crank speed fluctuations by assuming that high and low frequency information content would be available. These were used as input data to a complex radial basis function network, and verified on a 9 L, 4-stroke, 6-cylinder turbocharged diesel engine running on ethanol. Cylinder pressure was measured using a sensor mounted on Cylinder-1, with an

accelerometer mounted on a head bolt. Reconstruction results were very good for peak pressure, with an error of 1.8%, but a position of peak pressure error up to 5˚CA. Use of vibration signals and a radial basis function network was attempted in [18]. Experimental data was collected from a single cylinder diesel engine fitted with a pressure sensor and a capacitive accelerometer glued directly to the cylinder, just below the cylinder head. The models produced accurate results, with peak pressure errors less than 2.7%, and location of peak pressure less than 1.45°. The results appear to be the best example of neural network based cylinder pressure reconstruction on diesel engines. Successful Application of the same approach to a multi-cylinder diesel engine has been reported in [19]. Work in [20] used measured vibration signals and pattern recognition to describe the so called 'reciprocating inertia force excitation' (RIFE). As block vibration responds to both RIFE and cylinder pressures, subtraction of the RIFE from block vibration produces content that closely resembles the rate of cylinder pressure rise. Verification involved a single cylinder diesel engine fitted with a pressure sensor and a vibration velocity sensor mounted directly onto the surface of the cylinder. The vibration velocity with, and without RIFE were compared using the correlation coefficient between the rate of cylinder pressure rise and the vibration velocities. At low engine speed and zero torque, raw vibration velocity produced a correlation coefficient of 0.77 compared to processed results which produced a value of 0.86. However, the most noteworthy result was found at a speed of 1200 rpm, and load of 10 Nm, where the vibration velocity produced a correlation coefficient of 0.01 compared to the processed result of 0.93.

In this paper a unified approach is developed for cylinder pressure reconstruction using Time-Delay feed-forward Neural Networks which, for the first time, provides a single methodology suitable for both crank kinematics and knock sensor data. This involves optimized signal processing applied to reconstruction for steady-state engine conditions.

Both applications are examined, i.e. using crank kinematics (via a shaft encoder) and cylinder block vibration (via a knock sensor). The objective of the paper is to test the accuracy of the methodology using a range of data captured from a multi-cylinder engine.

2. CREATION OF A UNIFIED RECONSTRUCTION METHODOLOGY

This section creates the single pressure trace reconstruction methodology by first discussing feed-forward network configuration and training, then identifying existing shortcomings particularly with recurrent neural networks which use feedback for both crank kinematic and block vibration based reconstruction. A summarised procedure for the methodology is given at the end of the section.

Feedback has been increasingly used to improve the reconstruction capability because reconstructed pressure gives some indication of the magnitude of subsequent cylinder pressures, facilitating noise reduction and also providing internal memory. Feedback can also have a positive impact on the ability of a network to reconstruct however this impact is limited only to one region of the pressure trace: i.e. the point of ignition. From that point forward, cylinder pressure can vary significantly cycle-by-cycle where feedback will have less impact. As a result, despite considerable refinement effort, recurrent networks have unfortunately not delivered the accuracy and robustness required. Delays in either crank kinematics or block vibration responses, are actually more critical than feedback because they capture significant changes to the network input. A single methodology is created here by exposing the sources of earlier failure through careful examination and testing of both NARX (recurrent) models, and standard Time-Delay (feedforward) networks of the structure shown in Figure 1. Time-Delay network based cylinder pressure reconstruction using engine block vibrations and crank kinematics, are then compared. This comparison reveals important insight into: i) the effect of connecting rod inertia on reconstruction

accuracy, ii) the need to filter input data, and iii) the need to reconstruct pressure for individual cylinders. First, the basic equations associated with a time delay network prediction are given, followed by the Levenberg-Marquadt training algorithm. Then the limitations of recurrent networks for cylinder pressure reconstruction are identified culminating in the identification of four issues which are resolved by Time Delay networks.

2.1 Time Delay neural networks and Levenberg-Marquadt training.

The processing capability of a single neuron is now explained, and how a generalisation, in the form of a standard multilayer feedforward neural network, can be adapted to become a Time-Delay network such as shown in Figure 1. Feedforward networks can easily be trained using the Levenberg-Marquadt algorithm - this is also explained briefly.

An output variable y that results from passing a vector of input variables x_i into a single neuron with activation function φ, is given as:

$$y = \varphi(\sum_{i=1}^{n}(W_i x_i) + b) \quad (1)$$

where the activation function φ acts as a single neuron in a (single-layer) perceptron artificial neural network (ANN), W_i is a vector of input synaptic weights, and b is the neuron bias. The ability of a single neuron to successfully map a particular function is dependent on the values of the weights and the bias. This single neuron can be considered as 'feed-forward' because the information only flows in the forward direction. It is suitable for solving simple problems but is not suitable for complex mappings. To undertake complex mappings at least a multilayer perceptron is needed. A multilayer perceptron network with a single hidden layer acting on *n* inputs x_j, *j* =1,…,*n*, produces a mapping given by:

$$y = \varphi_o\left(\sum_{i=1}^{m}\left({}^{0}W_i(\varphi_i\left(\sum_{j=1}^{n}({}^{h}W_{ij}x_j) + b_i\right)\right) + b_0\right) \quad (2)$$

where y is the network output, *m* is the number hidden layer neuron activation functions φ_i

with an associated weight matrix ${}^{h}W_{ij}$ and bias vector b_i, φ_o is the output layer activation function with weight vector ${}^{0}W_i$ and bias b_0. The ability to handle complex mappings is dependent on the number of hidden layers and the number of neurons in each layer. This dependence is ultimately key to producing a good ANN model, achieved through successful training. Increasing the number of hidden layers and neurons, expands the network potential but this has a negative impact on training and processing speed. The network given by equation (2) still does not lend itself to the solution of time series problems because it does not have any internal memory, and no perception of time variations. When configured as a Time-Delay network however, it has both memory and a perception of time variation. The mapping then becomes:

$$y_k = \varphi_o\left(\sum_{i=1}^{m}\left({}^{0}W_i(\varphi_i\left(\sum_{j=1}^{n}({}^{h}W_{ij}x_{k-j+1}) + b_i\right)\right) + b_0\right) \quad (3)$$

which is achieved using equation (2) by creating *n* inputs from a single variable x_k (at discrete time *k)* by setting: $x_1 = x_k$, $x_2 = x_{k-1}$, … , $x_n = x_{k-n+1}$. By increasing the number of hidden layers to two, an extended version of equation (3) gives a functional representation of the network shown in Figure 1. A multilayer perceptron can also be configured as a 'futuristic' mapping, i.e. using the same parameter definitions and a single variable x_k. Thus by setting $x_1 = x_k$, $x_2 = x_{k+1}$, … , $x_n = x_{k+n-1}$, the mapping is:

$$y_k = \varphi_o\left(\sum_{i=1}^{m}\left({}^{0}W_i(\varphi_i\left(\sum_{j=1}^{n}({}^{h}W_{ij}x_{k+j-1}) + b_i\right)\right) + b_0\right) \quad (4)$$

Furthermore, by defining a multiple input feedforward network through the use of both time delays and future values of a single input variable (and by setting W_{i0}=0), a 2*n* input network can be constructed in the form:

$$y_k = \varphi_o\left(\sum_{i=1}^{m}\left({}^{0}W_i(\varphi_i\left(\sum_{j=-n}^{n}({}^{h}W_{ij}x_{k+j-1}) + b_i\right)\right) + b_0\right) \quad (5)$$

As feedforward networks, equations (3) or (4) can be trained using the Levenberg-Marquadt algorithm (LMA). This is an iterative method used mainly for minimising multi-

variable functions [22]. It also works extremely well for training feedforward networks. The LMA is a compromise between two well-established optimisation methods: Newton's method, and the Gradient Descent method. Newton's method converges rapidly near a local minimum but it can diverge. Gradient Descent by contrast is almost guaranteed to converge but is significantly slower. The optimum adjustment ΔW for a feedforward network using the LMA is given as:

$$\Delta W = [H + \mu I]^{-1} g \tag{6}$$

where H is the Hessian matrix, g is the gradient vector, I is the identity matrix, and μ is a regularising parameter defined in [22]. The gradient vector is the derivative of the cost function $\varepsilon_{av(W)}$ with respect to weight vector W i.e.:

$$g(W) = \frac{\partial \varepsilon_{av}(W)}{\partial W} = -\frac{1}{N} \sum_{i=1}^{N} [d(i) + F(x(i); W)] \frac{\partial F(x(i); W)}{\partial W} \tag{7}$$

where the cost function is:

$$\varepsilon_{av}(W) = \frac{1}{2N} \sum_{i=1}^{N} [d(i) + F(x(i); W)]^2 \tag{8}$$

N is the length of the training sample, d is the desired output, and $F(x; W)$ is the approximating function realised by the network with x being the input vector. The Hessian matrix associated with cost function equation (8) is defined as:

$$H(w) = \frac{\partial^2 \varepsilon_{av}(W)}{\partial W^2} = \frac{1}{N} \sum_{i=1}^{N} \left[\frac{\partial F(x(i); W)}{\partial W}\right] \left[\frac{\partial F(x(i); W)}{\partial W}\right]^T - \frac{1}{N} \sum_{i=1}^{N} [d(i) + F(x(i); W)] \frac{\partial^2 F(x(i); W)}{\partial W^2}$$

… (9)

The Hessian describes the local curvature of a multi-variable function making equation (9) extremely difficult in practice to compute. To overcome this problem, approximations to the Hessian matrix have been developed using the Jacobian matrix J:

$$J = \frac{\partial F(x(i); W)}{\partial W} \tag{10}$$

which is used several times in equation (9). To the overcome the difficulty in constructing the Hessian matrix in the LMA, the second term in equation (9) is ignored, and the Jacobian is inserted to approximate the Hessian matrix, namely:

$$H \approx JJ^T \tag{11}$$

producing an approximation to equation (6) as follows:

$$\Delta W \approx [JJ^T + \mu I]^{-1}\varepsilon_{av}J \tag{12}$$

The LMA is relatively easy to implement producing highly accurate training, and good generalisation capability but it may find a local minimum therefore several networks need to be trained (with different initial conditions) to attempt find the global minimum.

2.2 The limitations of recurrent networks in cylinder pressure reconstruction

Although recurrent networks which use feedback have been the dominant architecture examined to date, by careful consideration of key stages in the combustion process it can be shown that recurrent networks are actually not suitable for cylinder pressure reconstruction. Error reductions in recurrent generalisation over time have gone from 5.12% in [10] to 4.8% in [21]. These developments show a trend towards good reconstruction in the low pressure regions but significant errors are evident in the high pressure regions. Moreover there is a tendency for reconstruction to become unstable with only a small chance of returning to stability. It is also evident that the more time spent in optimising a network on training data, the smaller the improvement in generalisation performance. Recurrent architectures may actually cause unjustified complexity although the initial justification for the use of recurrent neural networks is wholly sound. Data requirements, for recurrent networks comprise two types of input: cylinder pressure feedback, and delays.

To further explain the reason why recurrent networks are of limited value in this application, consider reconstruction over four parts of a trace i.e.: i) prior to the ignition, ii)

at ignition, iii) immediately after the ignition, and iv) significantly after ignition. These parts are shown on Figure 2. First, prior to ignition, cylinder pressure is relatively consistent, cycle-by-cycle, since the compression is nearly identical under steady-state conditions., Pressure feedback therefore has little influence on the reconstruction in this region. Second, at ignition, crank kinematics and block vibration responses have not yet been influenced by the rise in cylinder pressure. Immediately after the start of ignition, both crank kinematics or engine block vibrations vary as the cylinder pressure rises. Pressure feedback contains only partial ignition information, the main part would still relate to the compression process. A significant duration after the start of ignition, both the crank kinematics and block vibration responses are fully influenced by combustion activity. Cylinder pressure feedback would then contribute to the reconstruction.

It is evident that in key regions of the trace, cylinder pressure feedback is not important. The network would then become a time-delay network. Feedback can be useful for the latter part of combustion but it can also generate reconstruction errors early in the combustion process, which may cause a recurrent network to go unstable [11]. Therefore over most of the trace, recurrent networks can be simplified to time-delay networks. However an important realisation is that in addition to the adoption of ‘delays’ in the input, time delay networks will also benefit significantly from the adoption of ‘future’ data input.

2.3 Addressing four issues to develop a unified reconstruction approach

The development of unified approach using time delay networks is now progressed by examining four issues: 1/ the optimum number of neurons and delays; 2/ a comparison of the same pressure trace reconstructed using synchronised crank kinematics and block responses; 3/ the role of crank inertia in causing loss of information at TDC; and 4/ the impact of using ‘future’ information on the accuracy of reconstruction.

Finding the optimum number of neurons and delays in a time-delay network

A study was initially undertaken to examine the rms error and training times associated with the number of neurons and delays. The accuracy of various time-delay networks was examined as a function of the computational training time for different numbers of neurons and delays. Figure 3 shows the network training error as a function of training time for increasing number of hidden layer neurons and increasing number of delays. The optimum network was selected by weighing-up the performance versus the computation time. The best architecture in terms of accuracy and efficiency i.e. producing very good generalisation performance but without excessive training computation time, was found (for a 3-cylinder 4-stroke DISI engine) to be a single hidden-layer Time Delay network with between 10 - 15 neurons in the hidden layer, and around 120 delays. The input delays here are actually expressed in the crank domain e.g. 120° CA. The use of crank domain delays will be explained later in the section within a summary of the unified procedure for an *N*-cylinder 4-stroke engine.

A comparison using synchronised crank kinematics and block responses

A comparison was undertaken to examine similarities in the location and magnitude of the reconstruction errors associated with a pressure trace reconstructed in two ways i.e. using synchronised crank kinematics, and second, using block vibration responses. Figure 4 shows a comparison between a target pressure trace and the reconstructed trace obtained using crankshaft kinematics and block vibration responses. An unexpected result is obtained in that there are great similarities between the block acceleration-based reconstruction and crank kinematics based reconstruction. The comparison between these two normally independent routes to reconstruction shows that not only are there similarities in the position of the errors, but also in their magnitude, which implies that there is some previously unknown common link between these two networks and their

corresponding data sets. Following extensive experimentation using different networks and training algorithms, it was concluded that the link cannot be network dependent. Therefore the similarity between the two different results must originate from the input data. The only possible source of such similarity is that the engine block acceleration is influenced by a non-pressure induced mechanism that also affects crank kinematics. Finding a mechanism that influences the reverse process is very unlikely thus the possibilities are significantly reduced.

The source of this common error is established as the influence of crank-angle-varying connecting rod inertia. Evidence to confirm this mechanism can be established by considering the way in which conrod inertia impacts on block acceleration. The conrod inertia about the crank axis, varies with crank angle as a result of the change in distance between the crank axis and the conrod centre of gravity. A crank angle dependent variation in the conrod inertia produces a fluctuation in the crank torque and rolling moment excitation of the engine block about the crank axis, a component of which, accelerates the block laterally. Figure 5 shows an example comparison of the normalised inertia-induced crank torque and the cylinder-pressure generated torque as a function of crank angle. This shows that at around TDC the inertia-induced crank torque totally dominates over the cylinder pressure generated crank torque. This dominance produces the same loss of information between gas pressure and the crank kinematic response and between gas pressure and the block vibration response. This loss of information at TDC could be potentially unfortunate because the gas pressure typically reaches its peak just a few degrees after TDC. To circumvent the problem, the effect of conrod inertia variation can be calculated and removed from any measured response signal. However such action is not necessary when the network architecture is of the form given by equation (5) which

includes in its input, both historical data (i.e. delays) and future data. The evidence to confirm this is now explained.

The impact of using future information on the accuracy of reconstruction.

When using delay data only, Figure 4 clearly shows the crank angle regions where crank kinematics are directly influenced by cylinder pressure. By additionally using ‘future’ information as inputs to a time delay network, regions of useful information are targeted with the aim of getting significantly better reconstructions. The ‘historical’ inputs contain information about the start of the combustion, whereas (it is initially conjectured) that ‘future’ input data contains information about the entire combustion process beyond TDC. In other words, the future information requirement is derived from noting that crank acceleration depends on the cylinder pressure at an earlier time. Therefore to obtain the cylinder pressure at a particular time, crank acceleration information at a later time is needed. This hypothesis is tested involving a time-delay network trained using the Levenberg–Marquardt algorithm. Initially 60° CA of ‘future’ information is selected. Figure 6 shows a comparison between the use of historical input data versus the use of combined future and historical input data (in a nominal time delay network where the input is ± 60° CA). This shows significant gains in accuracy as well as a qualitative improvement. The overall performance improvement goes from an error of 3.49 % to 2.15 % for the generalised RMSE. Further network optimisation showed that the best combination was actually produced with 120° CA of historical input and 120° CA of future input, i.e. centred symmetrically about TDC firing. The optimum total range of historical and future input data for a 3 cylinder engine is 240° CA i.e. a third of a cycle, the total duration of combustion. This duration is no coincidence and can be best explained by considering the influence cylinder pressure has on the crank kinematics. Throughout the 240° CA of a combustion event (within an individual cylinder) the majority of the variations in crank kinematics will be

a direct result of the firing cylinder. The influence of other cylinders will be relatively small. However the crank kinematics outside the 240° combustion window, will be greatly influenced by the compression and exhaust strokes of the other cylinders. The choice of ± 120° input range therefore focuses entirely on the relevant pressure trace and excludes any influences from other cylinders. Applying the same argument to a 6 cylinder 4-stroke engine would mean that the optimum input range would be ± 60° CA. The findings of all the examinations discussed are now brought together into a summarised unified procedure.

A summary of the unified procedure for an *N*-cylinder 4-stroke engine

1/ Whether using crank kinematics or block vibration information to reconstruct cylinder pressure, all data is initially pre-processed in the time domain. This depends on the type of data being used as follows: when using crank kinematics as input data, use crank velocity data associated with each cylinder pressure. Crank velocity data is not concatenated. Cylinder pressure traces for each cylinder are concatenated so that each complete cycle of 720° is reduced to a window 720°/*N* either side of TDC, which is then combined (for example for a 4-stroke I3 engine, the window is 240° CA i.e. 120° CA either side of TDC). Note: the reason why kinematic data is not concatenated, is because if it were, the future and historical delays outside of the window would not correspond to the current combustion event but rather, would be associated with previous and future cycles. Therefore, future and historical crank kinematics are appropriately-linked to pre-concatenated cylinder pressures. Figure 7 shows the process of concatenating segments of the pressure trace and the way corresponding crank velocity signals are linked.

2/ Filter out high frequencies from kinematic data associated with each cycle (to remove noise). Note: filtering takes place on a cycle-by-cycle basis. This is important because were multiple cycles to be used, the genuine cylinder pressure variability would be lost.

3/ Convert the data from the time domain to crank angle domain by interpolation.

4/ Select a Time-Delay neural network for reconstruction, using one hidden-layer for crank-kinematic-based reconstruction; or 2 hidden-layers for block-vibration-response-based reconstruction, both with 15 neurons in each hidden-layer, using 360/*N* historical delays and 360/*N* ‘future’ inputs. For example for a 4-stroke I3 engine, use 120 historical delays, and 120 ‘future’ inputs. The use of both time delay (historical) information, and future input information takes account of the inertial effects discussed earlier in this section.

5/ Truncate the cylinder the pressure data $\pm 360°/N$ CA either side of TDC (for example for a 4-stroke I3 engine, $\pm 120°$ CA either side of TDC). Then separately concatenate cylinder pressure data for each cylinder.

6/ Arrange for network delays to be chosen relative to the crank-base associated with the appropriate cylinder pressure, then randomise the order.

7/ Finally, train with the (standard) Levenberg-Marquardt algorithm, nominally using 1000 epochs.

3. THE ENGINE TEST FACILITIES AND DATA ACQUISITION SYSTEM

The engine selected to generate test data was a 4-stroke 3-cylinder inline direct injected spark ignition (DISI) gasoline engine mounted on a 130 kW dynamometer in a test cell. This was a prototype development engine (designed by Ford and Yamaha) that never actually went to production. It was very suitable as a data source because successive firings on a 3-cylinder cylinder are spaced by 240 CA˚ eliminating any combustion overlap. The head and block were aluminium, with 4 valves per cylinder and belt driven camshafts. The engine was fitted with swirl-control valves to enhance inlet air turbulence; EGR to control NO_x emissions; knock control using Bosch tuned-accelerometer type knock sensors; and a torsional vibration damper. No clutch was fitted since the dynamometer was connected directly to the flywheel via a compliant torsional coupling whose critical frequencies were fully understood. The key engine parameters are given in Table 1. The natural frequency of the engine-dynamometer was 16.5 Hz which, for 3 a cylinder engine, gave a critical speed of 660 rpm which was avoided during acquisition of the data. A McClure-type 130kW/7000 rev/min DC dynamometer was used which has a maximum motoring power of 100 kW, an armature inertia of 0.87 kgm^2 and a coupling torsional stiffness of 1260 Nm/rad. The dynamometer was mounted in a rotating frame; torque measurements were taken by a load cell on a moment arm.

Table 1. 3-Cylinder DISI Engine parameters

Engine Kinematic Parameters	Value
Number of Cylinders	3 Inline
Bore	79.0 mm
Stroke	76.5 mm
Swept Volume	1125 cc
Connecting Rod Length	137 mm
Piston Pin Offset	0.8 mm
Compression Ratio	11.5
Piston Mass	270 g
Connecting Rod Mass	395 g
Crankshaft Primary Inertia	0.02579 kgm^2
Flywheel Inertia	0.12021 kgm^2

The engine was controlled manually by setting speed or load first, then varying throttle angle. For all tests the load was kept constant and by varying the throttle, the engine speed fluctuated. Key measurements were obtained using Kistler type 6117BCD36 spark-plug mounted pressure sensors in each cylinder, a high resolution shaft encoder, a production Bosch knock sensor (fitted on the engine block) in addition to the knock sensor used for knock control, and a standard accelerometer also fitted on the block. The cylinder pressure sensors when connected to Kistler type 5044 charge amplifiers using low noise charge cables give an operational range of 0 to 150 bar. The pressure sensor inputs are individually set to the sensing charge sensitivities using an output gain of 10 bar/volt [21]

The crank kinematics were obtained using a crankshaft nose-mounted 3600 pulse Kistler type 2614A1 optical encoder (with TDC marker), securely fixed to the cylinder block to prevent any corruption of the crank kinematic signal by engine vibration. Since crank

speed and crank acceleration are obtained by differentiating crank angle, data sampling takes place in the time domain as explained shortly. The encoder signal is passed through a Kistler type 2614A4 pulse multiplier which results in two output signals. The first is a 1-pulse for each rotation which can be used as the TDC marker when aligning the rising edge of the TTL signal equal to TDC. The second signal produces 360 or 3600 pulses for each rotation where the first pulse equates to the TDC signal. The encoder is constructed to produce 360 genuine physical pulses per revolution but with the capability (using extrapolation) to produce a signal with 3600 pulses per revolution. To obtain derivatives of the crank kinematics using encoder data, detailed correction is generally needed [21].

The application of a standard knock sensor to reconstruct cylinder pressure from engine block vibrations is very appealing as they are now already installed on the majority of production gasoline engines. The use of the knock control sensor was found to be problematic, owing to insufficient signal strength for both the ECU and data acquisition. Therefore, the additional standard Bosch A-261-231-114 knock sensor was fitted to the intake side between Cylinder-2 and Cylinder-3. This position was selected primarily for convenience, as the optimum position for cylinder pressure reconstruction may differ. The optimum location for reconstruction in terms of signal quality is not generally optimum for knock detection. This may generally justify a compromise location. In addition to the engine block accelerations measurements via a knock sensor, a piezo-electric accelerometer was also fitted. Standard knock sensors include internal signal filters. Therefore an (instrument quality) Sensonics PZP1 piezo-electric accelerometer, with a frequency and load range of 0-29 kHz and 0-600 g respectively, was fitted to the exhaust side and mounted on a bolt boss, to measure unfiltered accelerations. An inductive probe was also used to measure crank twist. The kinematics gathered through the inductive probe were compared to the encoder data and found to confirm negligible twist [21]

Data Acquisition

To achieve accurate synchronous measurements of cylinder pressure, crank angle, and knock sensor responses, a dedicated National Instruments system was created. The data acquisition hardware comprised an NI PXI-1031 chassis and a NI PXI-8331 interface for Windows PC connectivity. This system contained two input modules: the NI PXI-6133 analogue input module, and the NI PXI-6602 counter or timer module. The NI PXI-6133 analogue input module captured data on 8 channels with 14-bit synchronous sampling. The analogue inputs were connected using low noise co-axial cables via a TB-2709 terminal block with max sampling rate of 2.5 MHz and max input amplitude of 10V. The high sampling rate and dynamic range of the NI PXI-6133 module is particularly suited to this application and is comparable to existing engine combustion data analysis systems. This module was used to acquire the data from all inputs except the crankshaft encoder TTL signal. The NI PXI-6602 counter module was used for 32-bit crank encoder signal capture with a maximum source frequency of 800 MHz. Again, this signal is transmitted through low noise co-axial cables and then into a BNC-2121 terminal block. The details of the data acquisition rates, noise suppression, and pegging of the cylinder pressure signals have been comprehensively described in [21]. Within most combustion analysis systems, data is acquired in crank domain, i.e. with constant crank angle. Bennett [21] argued that this would not be adequate as the sampling frequencies would vary with engine speed and, as there was no aliasing protection, there would be little confidence in producing uncorrupted low frequency data. Bennett [21] also came to the conclusion that the ANNs would train more successfully using time-based data rather than crank-angle-based data. The selection of time-based data acquisition would remove the need for re-sampling. The main initial concern using time domain sampling was synchronisation between the analogue inputs and the TTL signal from the crank encoder. This difficulty was overcome

in [21] by using the TDC pulse from the encoder to trigger the acquisition of all the inputs for each cycle. This method removes any drift in the acquisition data which could be compounded over many cycles.

The two most significant issues relating to the data acquisition hardware concern errors associated with the crank encoder and its need for calibration. The second is the non-physically derived 0.1˚ resolution of the Kistler encoder. First regarding the encoder errors, this arises because each of the 360 slits on the encoder disc were manufactured with a small random error so that they were not precisely 1˚. These errors are acceptable for measuring crank angle displacement but become a serious problem when the signal is differentiated numerically to obtain angular velocity, and angular acceleration. The problem was largely solved by calibration as now explained.

Obtaining crank velocity and acceleration by differentiating raw data from the Kistler crank encoder reveals a major problem. Velocity data is generally noisy, but is found to be cyclically repeatable. Differentiating velocity to obtain acceleration produces totally unacceptable results caused by significant high frequency corruption which is repeated over a revolution. This is caused by the degree marker spacings (on the encoder) not being manufactured to sufficient accuracy. Each 1° pulse appears to have a repeatable error. But as the encoder completes 360°, the error is reset.

A procedure that examines the ‘coast down’ of a free encoder mounted on a disc, has been developed to overcome the problem by calibrating the encoder. Transient calibration is necessary owing to the difficulty of obtaining perfectly constant speed. The procedure involves a disc of known inertia (e.g. 475×10^{-6} kgm^2) being attached to an otherwise free encoder (i.e. uncoupled from the engine). The disc is spun up to speed and allowed to coast down to rest under the action of friction. To measure disc-coast-down, the TTL signals from both the 1 ppr, and 360 ppr pulse trains, were captured via the NI data

acquisition system using 80MHz counters to fix the sampling rate. The angular displacement corresponding to the 1 ppr signal was assumed to be error free because the same optical slot is used in the encoder disc (when the pulse is 360° apart). Defining the time interval between the actual measured TTL pulses as t_{TTL}, the error ε_i can then be estimated for i=1°,…,360° where $\varepsilon_i = \omega_i (t_{\text{int}} - t_{TTL})$. To model the time when the 1° spaced pulses should appear, a cubic spline is fitted to the data. The encoder error, that must be re-calibrated, is the difference between the times predicted by the spline and the measured 360 ppr TTL signal. By repeating over 10 revolutions, a set of final calibration values is created which are then used to calculate the crank velocity, instead of using the nominal 1° values. Smooth angular velocity histories are obtained, which can be numerically differentiated again to obtain crank acceleration giving a significant improvement in signal-to-noise ratio compared to the use of raw data.

With regard to the non-physical encoder resolution of 0.1˚ for the 3600 ppr encoder, it was found that the encoder actually used the two previous positions and extrapolated forward assuming little had changed. As a result, the 0.1˚ was not a genuine physical measurement therefore the high resolution signal was not used.

The engine data selection was chosen to represent real operating conditions. Low-speed low-load conditions were deemed most useful owing to high cycle-to-cycle variability which makes cylinder pressures less predictable. Three different speed conditions were selected for data capture: 1000 rpm, 1500 rpm, and 2000 rpm, along with three different load torques: 10 Nm, 20 Nm, and 30 Nm. Speed ramp information was also acquired at fixed torque of 20 Nm by varying throttle position to increase speed from 1000 rpm to 1500 rpm, and from 1000 rpm to 2000 rpm over a 60 second period. Steady state engine conditions relevant to reconstruction using both crank kinematics and block vibration responses are given in Table 2.

Table 2. Test conditions used for assessing cylinder pressure reconstruction

Condition	1	2	3	4	5	6	7	8	9
Engine Speed (rpm)	1000	1500	2000	1000	1500	2000	1000	1500	2000
Engine Load (Nm)	10	10	10	20	20	20	30	30	30
Nominal Engine Power (kW)	1.05	1.57	2.09	2.09	3.14	4.19	3.14	4.71	6.28

For each of the conditions given in Table 2 multiple sets of synchronised cylinder pressures on all cylinders, and corresponding crank positions, knock responses, and block accelerations were captured and processed into high fidelity time, and crank domain signals. This data is used in Sections 4 and 5 for crank and block-based reconstruction.

4. APPLICATION OF THE UNIFIED APPROACH TO CRANK KINEMATICS

The unified neural network based reconstruction procedure of Section 2 is now applied to crank kinematic based reconstruction. In total, all 9 conditions in Table 2 were used to train Time-Delay networks and then to test them under generalisation conditions (i.e. using the same condition, but a totally different set of data from the training set). For each of the 9 conditions in Table 2, a sufficient number of different networks were trained to enable repeatability statistics to be established. The ‘best’ trained network, in terms of lowest root mean square error (for each condition), was then adopted for generalisation at that condition. Table 3 shows the overall generalisation performance over 180 cycles of data using the ‘best’ trained network appropriate for each of the 9 test conditions. The Root Mean Square Error (RMSE) is defined as the square root of the mean of the squared error between the complete generalised reconstruction and the measured cylinder pressure. The Normalised Peak Error is the ratio (as a percentage) of the error between the reconstructed peak pressure and the measured cylinder pressure divided by the maximum measured cylinder pressure for that condition.

Table 3. Generalisation performance for each of the 9 Crank Test Conditions involving 180 engine cycles.

	Overall Performance (RMSE)	Normalised Peak Error	Peak Pressure Position Error (deg)
Condition-1	1.14 %	2.80 %	2.24
Condition-2	1.32 %	1.76 %	1.65
Condition-3	1.24 %	1.52 %	1.64
Condition-4	1.15 %	2.48 %	3.08
Condition-5	1.21 %	2.60 %	1.91
Condition-6	1.34 %	1.84 %	1.73
Condition-7	1.32 %	2.56 %	1.78
Condition-8	1.30 %	2.86 %	2.24
Condition-9	1.24 %	2.08 %	1.55

In addition to testing the overall generalised performance of each of the ‘best’ networks over 180 cycles in each of the Conditions 1 – 8, testing also examined the performance for individual cycles throughout the entire data set. By doing this, it is possible to identify cycles for which the prediction error can be classed as relatively ‘good’, ‘moderate’, or ‘poor’ (even if the error associated with relatively ‘poor’ cases is actually still very low). Figure 8 shows for Condition-1, a generalisation prediction classed as ‘moderate’ for which the normalised root mean square error (RMSE) was 1.25%. In Condition-1, there were some sets of predictions that were actually better, and some that were worse but overall, all of the results can be classed as very good, some being outstanding. Figure 9 and Figure 10 show corresponding ‘moderate’ generalisation predictions for Condition-5, and Condition-9 for which the RMSE values are 0.79% and 1.24% respectively.

Discussion of Crank-based reconstruction results

It can be seen from Table 3 that both sets of errors i.e. associated with the normalised peak pressure, and the position of peak pressure, appear to be fairly random and have no

discernible dependence on increasing power. Also Table 3 shows that the level of cycle-by-cycle variability has no impact on the reconstruction capability. The errors, associated with the best performing networks used to generate the results in Table 3, are very small, which demonstrates that using crankshaft kinematics, cylinder pressure can be reconstructed to a very high degree of accuracy under general conditions. It is also found that the most significant errors are not restricted to the peak cylinder pressure but rather are distributed across the entire pressure profile. This vindicates the use of 'future' and 'historical' input data, as described in Section 2, showing that it has the desired effect of reconstructing cylinder pressure rather than system inertia.

Other results used to generate the results in Table 3 (but not shown in detail) confirm the ability to reconstruct the cylinder pressure for abnormal or uncommon combustion activity, in particular, showing that the trained network is able to recognise in the crank kinematics that a combustion event differs from the average. Importantly, there was no evidence of instability or occasional peak pressure errors. Overall the results are a significant improvement over all published crank kinematic based results.

With regard to the computational effort required for training, using 240 inputs, and 15 neurons (with 3,631 weights and more than 30,000 data points) the average network training time (using Matlab on a desk-top PC) was less than 30 minutes. This is a marked improvement over the training efficiencies associated with recurrent networks.

5. APPLICATION OF THE UNIFIED APPROACH TO BLOCK VIBRATIONS

This section gives detailed results of applying the same methodology used in Section 4 to reconstruct cylinder pressure using engine block vibration measurements. The methodology is essentially the same although there are two necessary modifications to achieve the same level of accuracy achieved with crank kinematics. One main difference for block vibration based reconstruction is that there is greater information content in a

block vibration signal subsequent to the occurrence of peak pressure because pressure-related vibrations have to travel some distance before reaching a measurement point (e.g. an accelerometer). Similarly, there are differences in the vibration path distances for each of the three cylinders. Therefore even though filtering within the cycle is still appropriate for block vibration based reconstruction, many more frequencies need to be filtered. Whereas the frequencies associated with cylinder pressure traces and crank kinematics are similar, the relationship between the cylinder pressure and engine block vibration is significantly more complex. Frequencies associated with engine block vibrations are significantly higher, in fact, it is not unusual for vibration frequencies to exceed 10 kHz. Network training up to these frequencies would require a very large number of hidden-layer neurons – as a consequence training using raw vibration signals is generally not practical. A modification to the cut-off frequency is therefore needed because various non-pressure events contribute to block vibration signals, such as valve and injector activity [23]. The selection of the cut-off frequency is critical for successful training and reconstruction. It is therefore chosen by considering knock frequencies, typically above 6 kHz. There should not be any important cylinder pressure related vibration information at or above the knock frequency. This was therefore selected as the low-pass filter cut-off frequency.

A modification was also required to the ANN structure to take into account how the number of hidden layers and neurons are dependent on the complexity of the problem. Tests using the same basic structure as for crank kinematics based reconstruction were not good: i.e. using a single hidden layer with 15 neurons. By increasing the number of hidden layers to two, each having 15 neurons, proves very effective in terms of reconstruction accuracy without the need to significantly increase the training time. For the 3-cyinder 4-stroke test engine, the ANN had 240 input delays, where 120 were

dedicated to the 'historical' inputs, and 120 were dedicated to the 'future' inputs. The Levenberg-Marquardt training algorithm was used with a mean squared error cost function, and a maximum epoch number of 1000.

Regarding the test conditions for block-vibration-based reconstruction, the same 9 conditions shown in Table 2 were examined allowing the accuracy associated with each trained network to be shown in Table 4 corresponding to 180 cycles of generalisation data. And in a similar way to crank-based reconstruction, block-vibration-based reconstruction testing also examined the performance for individual cycles throughout the entire data set This again enabled identification of cycles with a prediction error that can be classed as relatively ‘good’, ‘moderate’, or ‘poor’ (again recognising that the error for a relatively ‘poor’ case may still actually be very small).

Table 4. Generalisation performance for each of 9 Block Vibration Test Conditions involving 180 engine cycles.

	Overall Performance (RMSE)	Normalised Peak Error	Peak Pressure Position Error (deg)
Condition-1	2.72 %	9.69 %	2.16
Condition-2	1.32 %	3.14 %	1.31
Condition-3	1.94 %	3.68 %	1.57
Condition-4	3.46 %	13.2 %	5.01
Condition-5	2.61 %	8.60 %	1.71
Condition-6	2.02 %	2.99 %	0.91
Condition-7	1.88 %	5.17 %	1.83
Condition-8	4.33 %	14.1 %	4.79
Condition-9	1.98 %	3.14 %	1.06

Figure 11 shows a comparison of reconstruction for Condition-1 using block-vibration inputs in generalisation for which an RMSE of 2.07% can be classed as relatively

‘moderate’. Figure 12 shows a ‘moderate’ generalisation results for Condition-5 with an RMSE of 2.82%. And Figure 13 shows a ‘moderate’ Condition-9 generalisation with an RMSE of 1.48%.

Discussion of results

It can be seen from the results that the reconstruction performance seems to be condition dependent but there is little evidence that variability impacts on the reconstruction accuracy. At similar speed or load conditions the results can be quite different which is believed to be noise on the input data rather than a flaw in the reconstruction methodology. Overall, Table 4 and Figures 11, 12, and 13 demonstrate that the cylinder pressure can be successfully reconstructed using engine block vibration under general conditions. Again, errors are also spread along the entire pressure trace and not confined to peak pressure. This confirms that the use of 'future' and 'historical' inputs, has the desired effect in accurately reconstructing using block vibrations. Several noteworthy reconstruction results show the ability of a network to reconstruct cylinder pressure from abnormal or uncommon combustion events. An interesting finding during testing is that networks trained using the proposed unified methodology applied to block vibration information, do not necessarily reconstruct the most accurate cylinder pressure but they do recognise that the combustion event differs from the average, and as consequence, produce reasonably accurate reconstruction.

The overall generalisation results using block vibration-based reconstruction are much improved on previous published results and give very little evidence of the instability or significant peak pressure errors. With regard to the computational effort needed for training, using 240 inputs for example, with two hidden layers, each having 15 neurons (involving 3631 weights and more than 30000 data points) the average training time using standard Matlab toolbox functions on a standard desk-top PC was 44 minutes.

6. CONCLUSIONS

A single approach to cylinder pressure reconstruction using crank kinematics or block vibration has been developed using Time-delay feed-forward Neural Networks. This involves optimized signal processing applied to reconstruction for steady-state engine conditions using a network trained with the standard Levenberg-Marquardt algorithm. The methodology has been tested using synchronous data captured from a 3-cylinder in-line DISI engine based on crank velocity obtained via a shaft encoder, and block vibrations in the form of measured accelerations obtained with a knock sensor. The results for crank kinematic based reconstruction using 200 cycles are highly accurate, with peak pressure errors consistently between 1.14% and 1.34%, demonstrating that cycle-by-cycle cylinder pressure variability has no effect on accuracy. The results using engine block vibration responses also have very acceptable accuracy with errors between 1.32% and 4.33%. Overall, peak pressure is more accurately predicted via crank kinematics whereas the position of peak pressure is more accurately predicted via block vibration measurements.

Acknowledgements
The authors wish to acknowledge funding support for this project from both the EPSRC and Jaguar Land Rover, under Contract Number: EP/E03246X/1. The considerable technical support is acknowledged of colleagues at Powertrain Research & Technology - Jaguar Land Rover, Coventry, and earlier, at Jaguar Land Rover - Advanced Powertrain Engineering, Whitley Engineering Centre, Coventry.

References

[1] Kolbeck, A. 2011. Closed loop combustion control - Enabler of future refined engine performance regarding power, efficiency, emissions & NVH under stringent governmental regulation. SAE International, (2011-24-0171).

[2] Rackmil, C and McKay, D. 2010. Sensor-less individual cylinder pressure estimation and closed loop combustion control for cold starts and torque balancing. SAE International, (2010-01-1269).

[3] Larsson, S. & Schagerberg, S. 2004. SI-Engine Cylinder Pressure Estimation using Torque Sensor, SAE Paper No. 2004-01-1369.

[4] Rizzoni, G, 1989. Estimate of indicated torque from crankshaft speed fluctuations: a model for the dynamics of the IC engine. IEEE Transactions on Vehicular Technology, Vol. 38

[5] Shiao, Y. and Moskwa, J., 1994. Misfire Detection and Cylinder Pressure Reconstruction for SI Engines, SAE Technical Paper 940144.

[6] Lim, B., Lim, I., Park, J., Son, Y. et al. 1994. Estimation of the Cylinder Pressure in a SI Engine Using the Variation of Crankshaft Speed," SAE Technical Paper 940145.

[7] Gu, F., Jacob, P.J and Ball, A.D. 1996. A RBF neural network model for cylinder pressure reconstruction in internal combustion engines. IEE Colloquium on Modeling and Signal Processing for Fault Diagnosis No.260 pp.4/1 - 4/11.

[8] Jacob, P.J., Gu, F. and Ball, A.D. 1999. Non-Parametric models in the monitoring of engine performance and condition. Part 1: modelling of non-linear engine processes". Proc. Instn Mech. Engrs Part D of Journal of Automotive Engineering Vol. 213, No. D1, pp. 73-81.

[9] Gu, F., Jacob, P.J and Ball, A.D. 1999. Non-Parametric models in the monitoring of engine performance and condition. Part 2: Non-intrusive estimation of diesel engine cylinder pressure and its use in fault detection". Proc. Instn Mech. Engrs Part D of Journal of Automotive Engineering Vol. 213, No. D3, pp. 135-143.

[10] Hamedovic, H., Raichle, F., Breuninger, J., Ficher, W., Dieterle, W., Klenk, M. and Böhme, J.F. 2005. IMEP-estimation and in-cylinder pressure reconstruction for multicylinder SI-engine by combined processing of engine speed and one cylinder pressure. SAE International, (2005-01-0053).

[11] Potenza, R., Dunne, J.F., Vulli, S., Richardson, D and King, P. 2007. Multicylinder engine pressure reconstruction using NARX neural networks and crank kinematics. International Journal of Engine Research, Vol. 8 (6). pp. 499-518.

[12] Weißenborn, E., Bossmeyer, T. & Bertram, T. 2011. Adaptation of a zero-dimensional cylinder pressure model for diesel engines using the crankshaft rotational speed. *Mechanical Systems and Signal Processing* 25 (2011) 1887–1910.

[13] Saraswati, S and Chand, S. 2010. Reconstruction of cylinder pressure for SI engine using recurrent neural network. Neural Computing and Applications, Springer, Vol 19(6), 935-944.

[14] Mocanu, F and Taraza, D. 2013. Estimation of main combustion parameters from the measured instantaneous crankshaft speed. SAE International, (2013-01-0326).

[15] Taglialatela, F. Lavorgna, M. Mancaruso, E. and Vaglieco, B.M. 2013. Determination of combustion parameters using engine crankshaft speed. Mechanical Systems and Signal Processing. Vol. 38 pp. 628–63.

[16] Villarino, R. and Böhme, J.F. 2003. Fast in-cylinder pressure reconstruction from structure-born sound using the EM algorithm. IEEE International Conference on Acoustics, Speech, and Signal Processing. Vol.6. pp. VI-597-600.

[17] Johnsson, R. 2006. Cylinder pressure reconstruction based on complex radial basis function networks from vibration and speed signals. Mechanical Systems and Signal Processing. Vol. 20 pp. 1923–1940.

[18] Bizon, K., Continillo, G., Mancaruso, E., and Vaglieco, B.M. 2011. Reconstruction of in-cylinder pressure in a diesel engine from vibration signal using RBF neural network models. SAE International, (2011-24-0161).

[19] Bizon, K., Continillo, G., Mancaruso, E., and Vaglieco, B. 2013. Towards On-Line Prediction of the In-Cylinder Pressure in Diesel Engines from Engine Vibration Using Artificial Neural Networks. SAE Technical Paper 2013-24-0137.

[20] Zhao, C., Cheng, Y., and Wang, L. 2014. Pattern recognition method applied to extract in-cylinder pressure excitation a response from measured vibration signals. SAE Technical Paper. 2014-01-2703.

[21] Bennett C. 2014. Reconstruction of Gasoline Engine In-Cylinder Pressures Using Recurrent Neural Networks, PhD Thesis, University of Sussex.

[22] Haykin, S. 2008 *Neural Networks and Learning Machines* (Third Edition), Prentice Hall.

[23] Vulli, S., Dunne, J. F., Potenza, R., and Richardson, D., King, P. 2009 Time-Frequency Analysis of Single- Point Engine-Block Vibration Measurements for Multiple Excitation-Event Identification, *Journal of Sound and Vibration*, 321, 1129-1143.

List of Figure Captions

Figure 1. Time-Delay Network Architecture with two hidden layers

Figure 2. Pressure Event Diagram: Region 1: prior to the ignition, Region 2: at ignition, Region 3: immediately after the ignition, and Region 4: significantly after ignition.

Figure 3. Network Training error as a function of training time for increasing number of hidden layer neurons and increasing number of delays.

Figure 4. Reconstructed and target pressure trace for 1000 rpm and 10 Nm obtained using crankshaft kinematics and block vibration responses. Top: Target pressure (grey continuous line), reconstructed with crankshaft kinematics (black dash dot line), and reconstructed with block accelerations (black dotted line); Middle: Corresponding crank velocity; Bottom: Corresponding block accelerations.

Figure 5. Dominance of the inertia relative to the cylinder pressure. Black dot dash line is the normalised crankshaft torque. Grey solid line is the normalised cylinder pressure torque.

Figure 6. Generalised cylinder pressure predictions using both future and historical data (black dotted line), versus historical data only (black dash dot line), compared with the corresponding measured cylinder pressure trace (grey continuous line).

Figure 7. Concatenation of the segments of pressure trace and the way that corresponding crank velocity signals are linked.

Figure 8. Condition-1 Crank-based Generalisation Results – 'moderate' case. Measured Cylinder Pressure (Grey Solid Line). Reconstructed Cylinder Pressure (Black Dashed Line). RMSE = 1.25%.

Figure 9. Condition-5 Crank-based Generalisation Results –'moderate' case. Measured Cylinder Pressure (Grey Solid Line). Reconstructed Cylinder Pressure (Black Dashed Line). RMSE = 0.79%.

Figure 10. Condition-9 Crank-based Generalisation Results –'moderate' case. Measured Cylinder Pressure (Grey Solid Line). Reconstructed Cylinder Pressure (Black Dashed Line). RMSE = 1.24%.

Figure 11. Condition-1 Block Vibration Generalisation Results –'moderate' case. Measured Cylinder Pressure (Grey Solid Line). Reconstructed Cylinder Pressure (Black Dashed Line). RMSE = 2.07%.

Figure 12. Condition-5 Block Vibration Generalisation Results –'moderate' case. Measured Cylinder Pressure (Grey Solid Line). Reconstructed Cylinder Pressure (Black Dashed Line). RMSE = 2.82%.

Figure 13. Condition-9 Block Vibration Generalisation Results –'moderate' case. Measured Cylinder Pressure (Grey Solid Line). Reconstructed Cylinder Pressure (Black Dashed Line). RMSE = 1.48%.

Figures

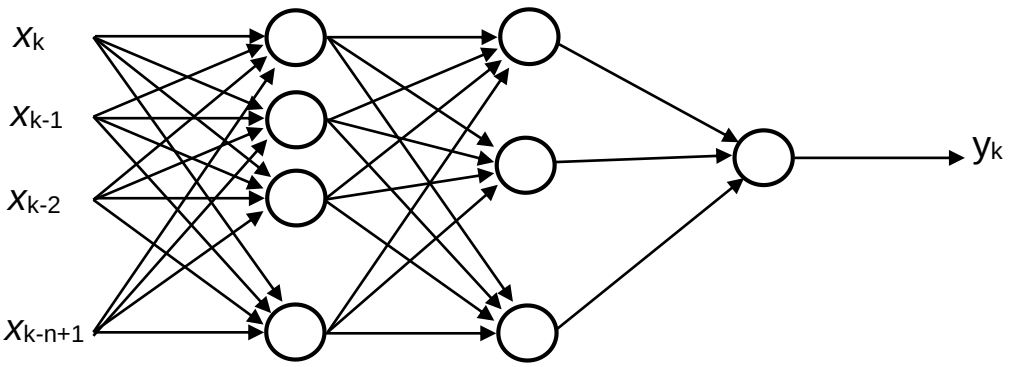

Figure 1. Time-Delay Network Architecture with two hidden layers

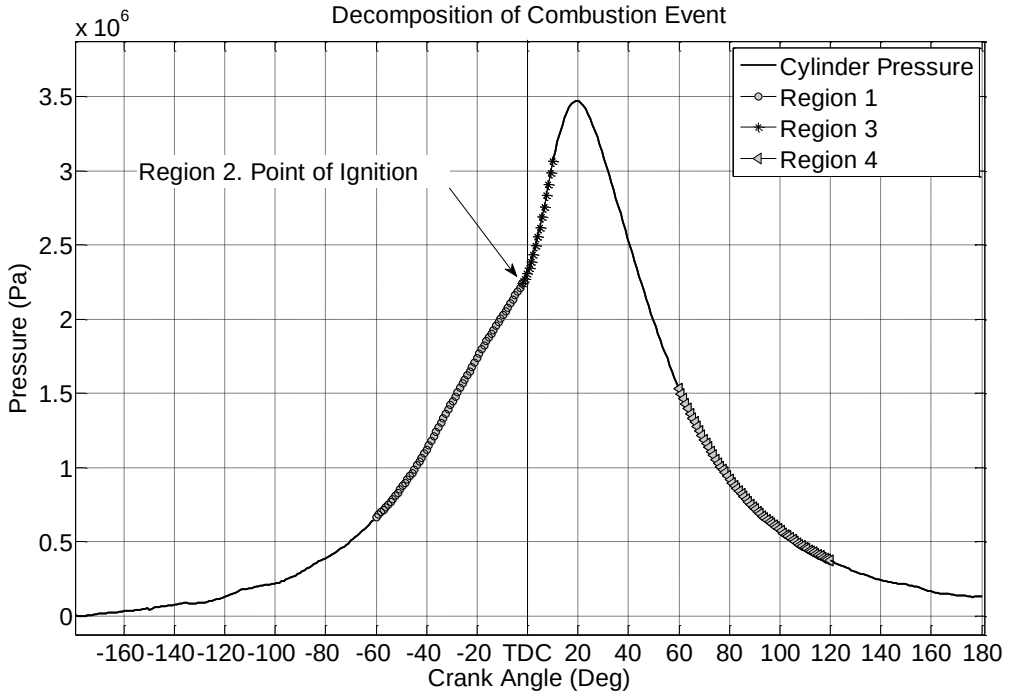

Figure 2. Pressure Event Diagram: Region 1: prior to the ignition, Region 2: at ignition, Region 3: immediately after the ignition, and Region 4: significantly after ignition.

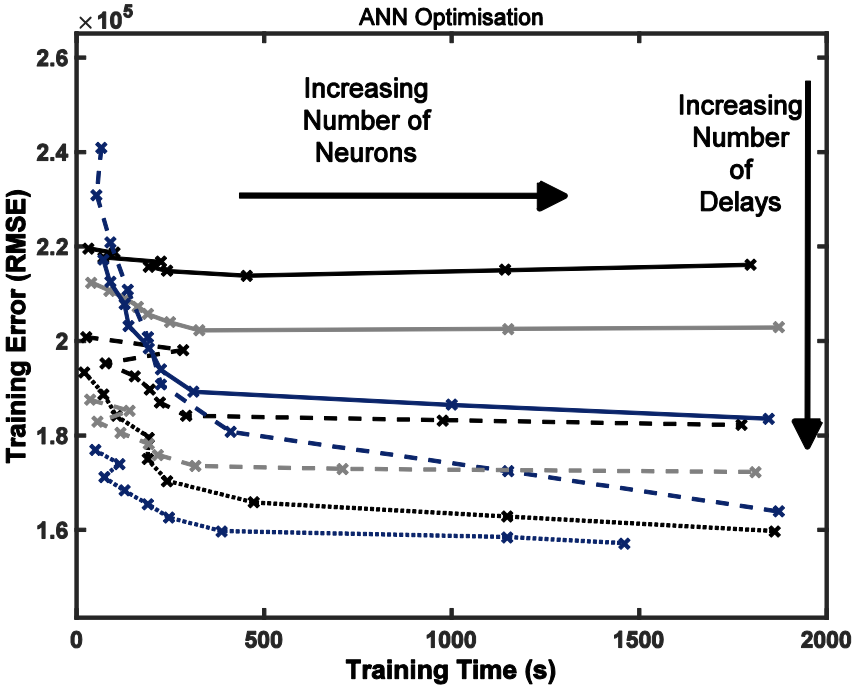

Figure 3. Network Training error as a function of training time for increasing number of hidden layer neurons and increasing number of delays

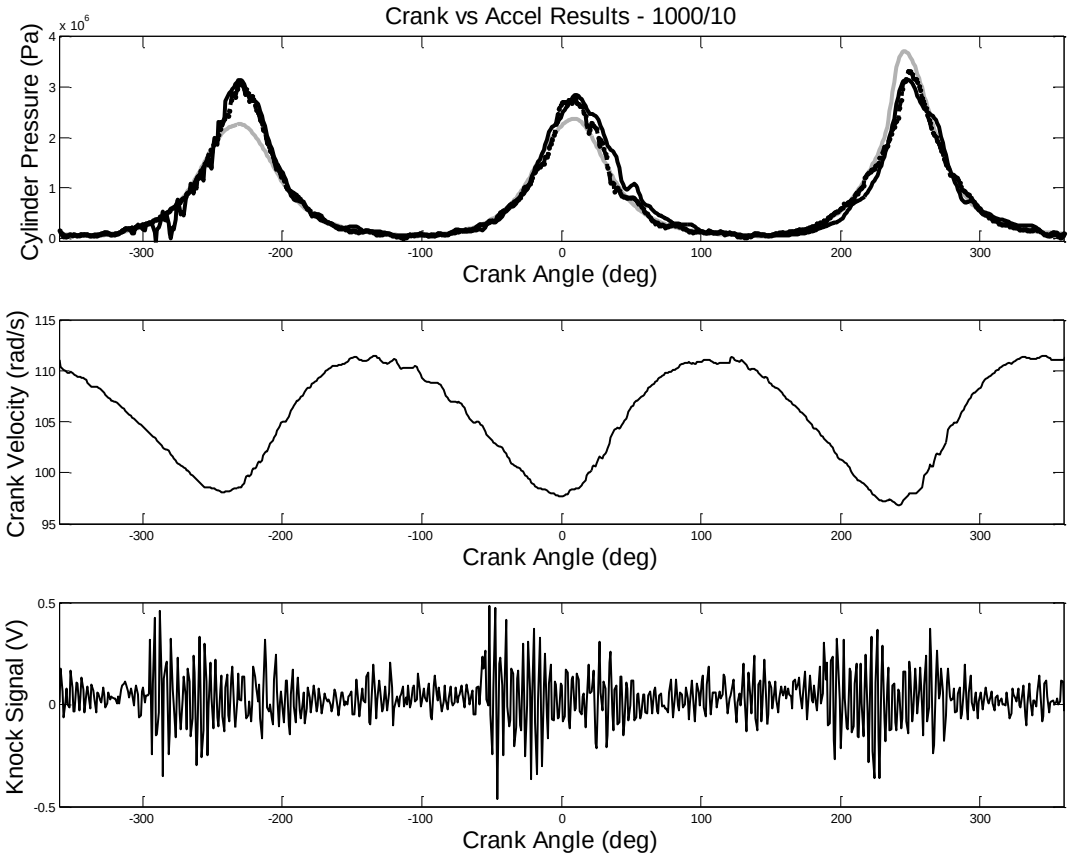

Figure 4. Reconstructed and target pressure trace for 1000 rpm and 10 Nm obtained using crankshaft kinematics and block vibration responses. Top: Target pressure (grey continuous line), reconstructed with crankshaft kinematics (black dash dot line), and reconstructed with block accelerations (black dotted line); Middle: Corresponding crank velocity; Bottom: Corresponding block accelerations.

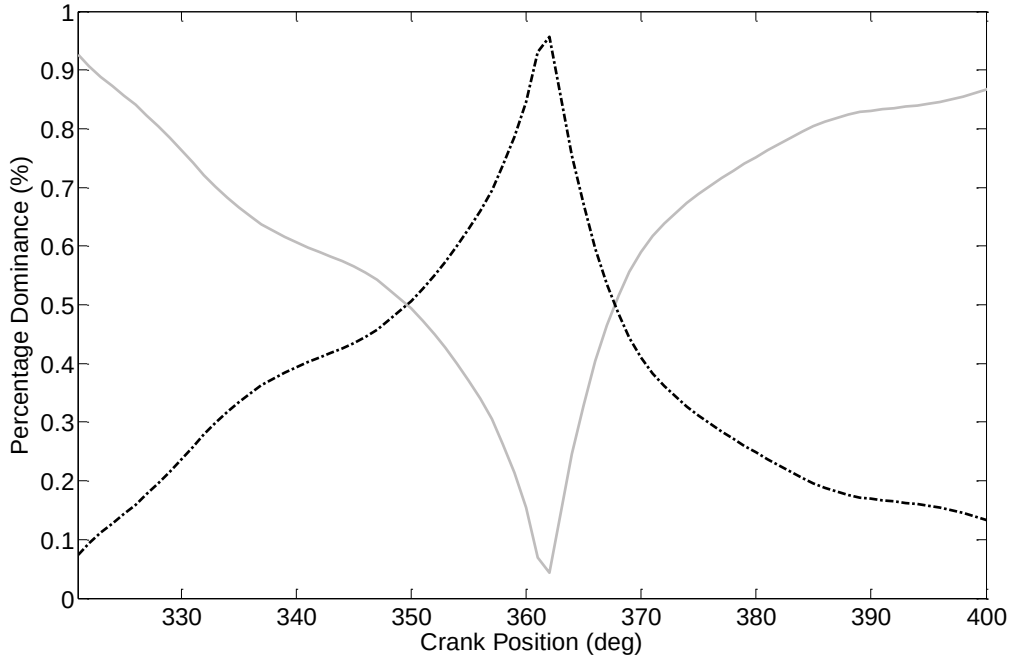

Figure 5. Dominance of the inertia relative to the cylinder pressure. Black dot dash line is the normalised crankshaft torque. Grey solid line is the normalised cylinder pressure torque.

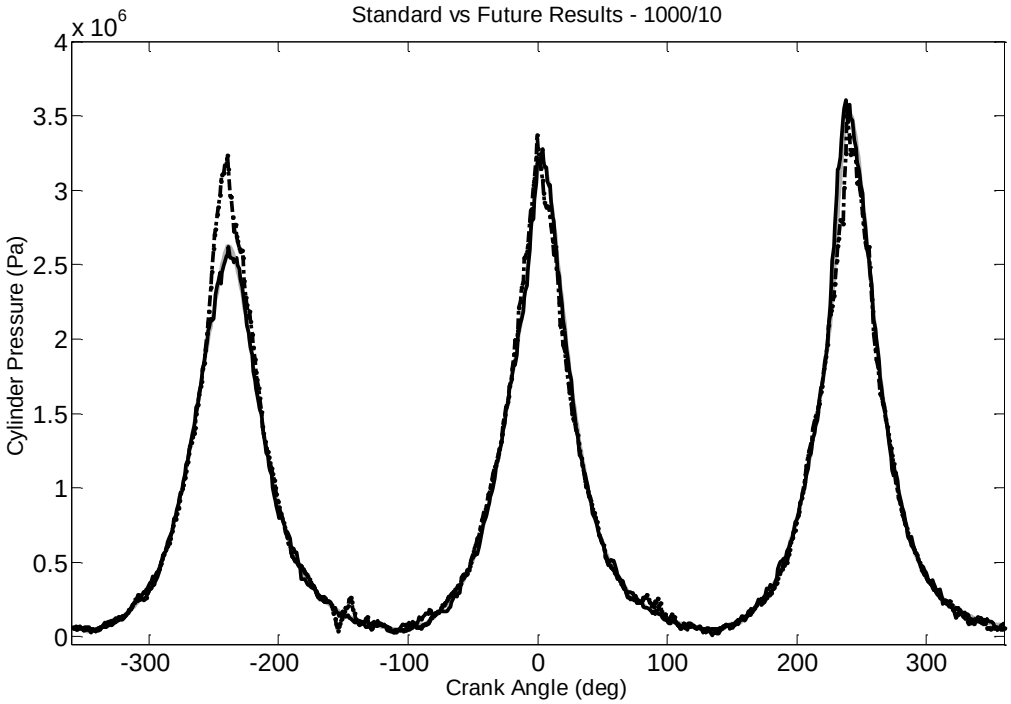

Figure 6. Generalised cylinder pressure predictions using both future and historical data (black dotted line), versus historical data only (black dash dot line), compared with the corresponding measured cylinder pressure trace (grey continuous line).

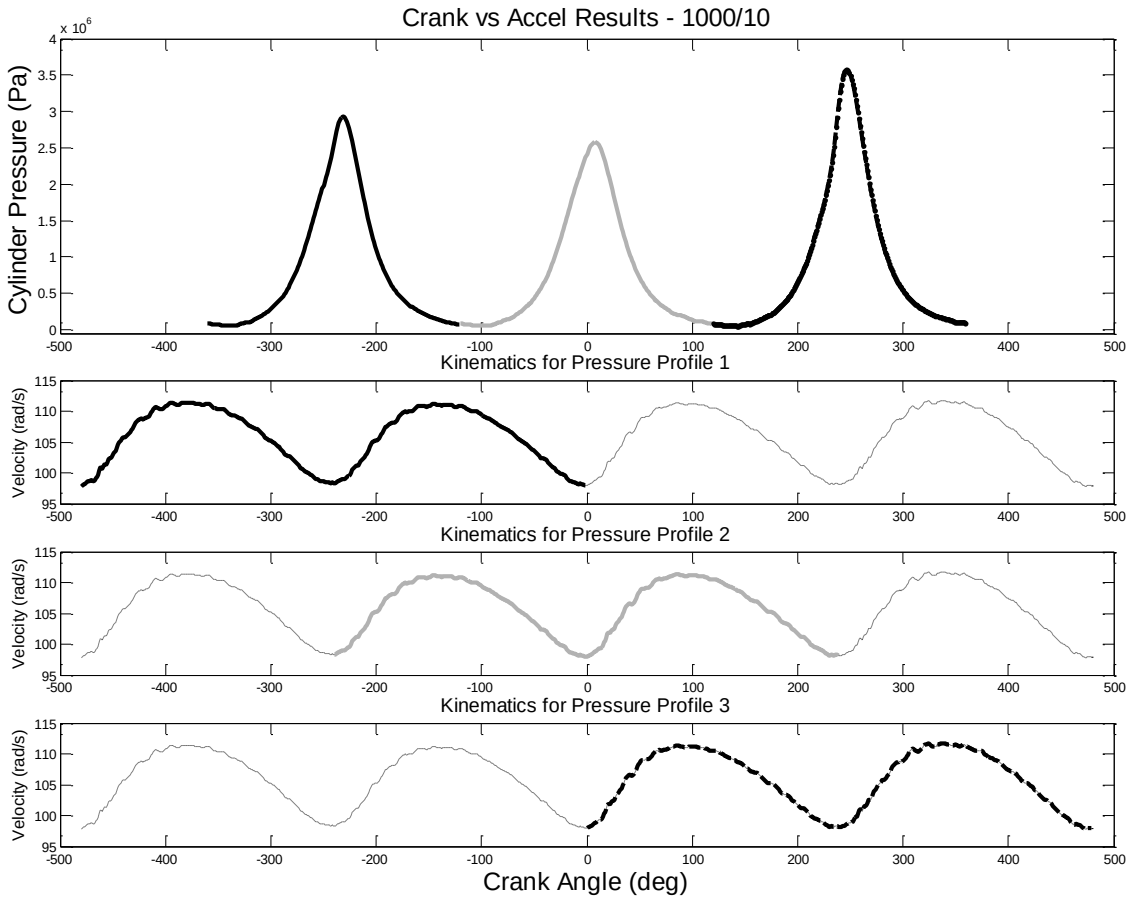

Figure 7. Concatenation of the segments of pressure trace and the way that corresponding crank velocity signals are linked.

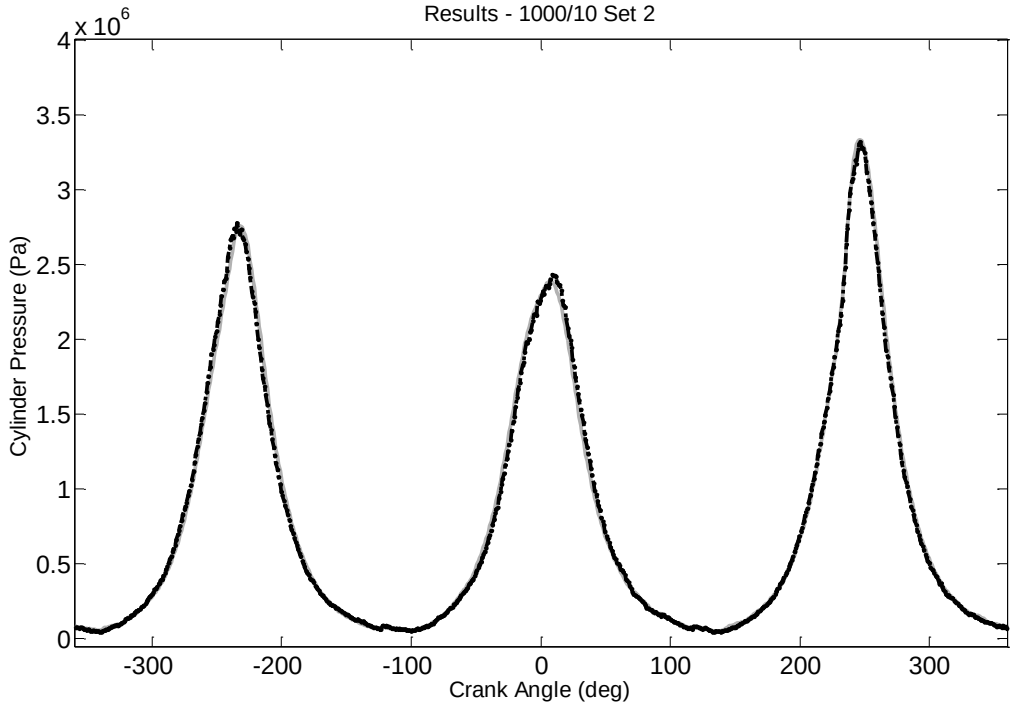

Figure 8. Condition-1 Crank-based Generalisation Results –'moderate' case. Measured Cylinder Pressure (Grey Solid Line). Reconstructed Cylinder Pressure (Black Dashed Line). RMSE = 1.25%.

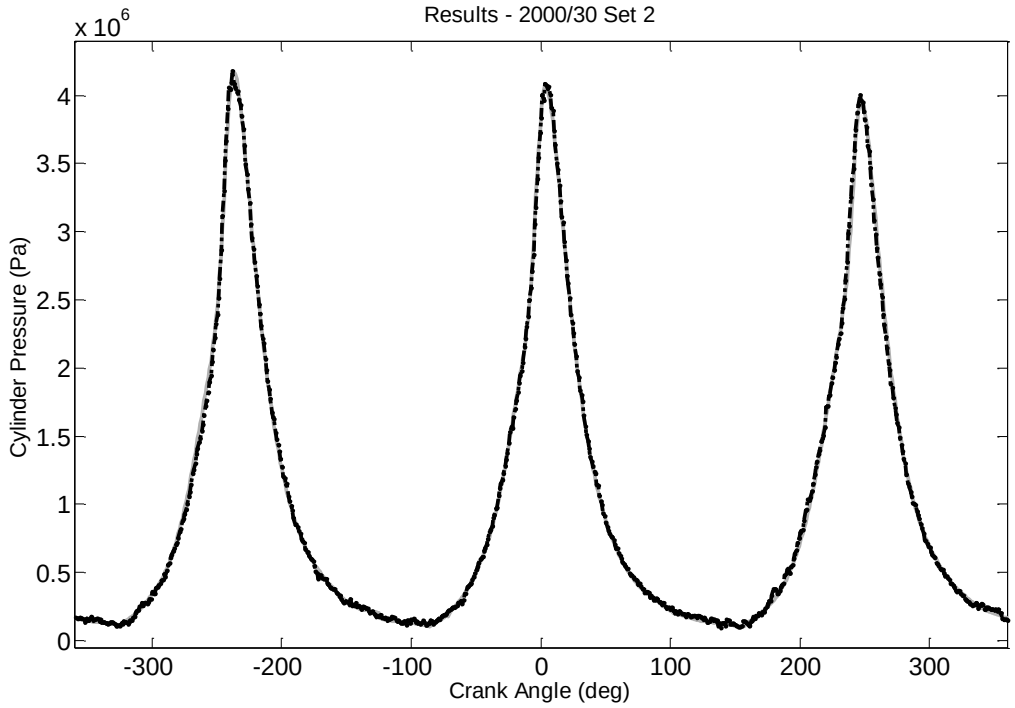

Figure 9. Condition-5 Crank-based Generalisation Results – 'moderate' case. Measured Cylinder Pressure (Grey Solid Line). Reconstructed Cylinder Pressure (Black Dashed Line). RMSE = 0.79%.

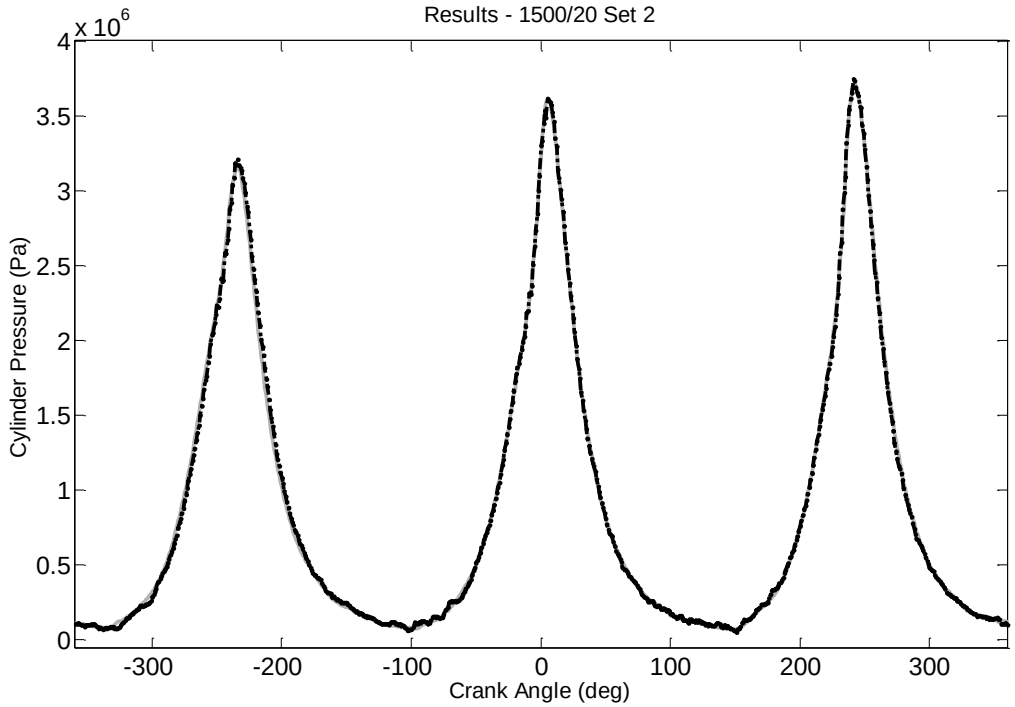

Figure 10. Condition-9 Crank-based Generalisation Results –'moderate' case. Measured Cylinder Pressure (Grey Solid Line). Reconstructed Cylinder Pressure (Black Dashed Line). RMSE = 1.24%.

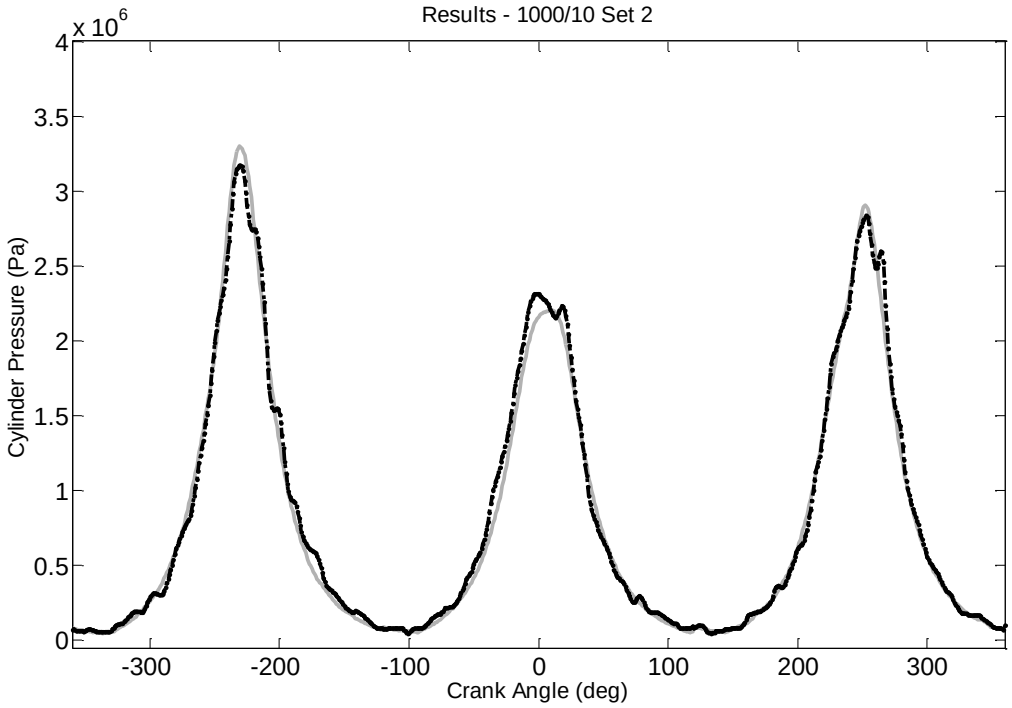

Figure 11. Condition-1 Block Vibration Generalisation Results – 'moderate' case. Measured Cylinder Pressure (Grey Solid Line). Reconstructed Cylinder Pressure (Black Dashed Line). RMSE = 2.07%.

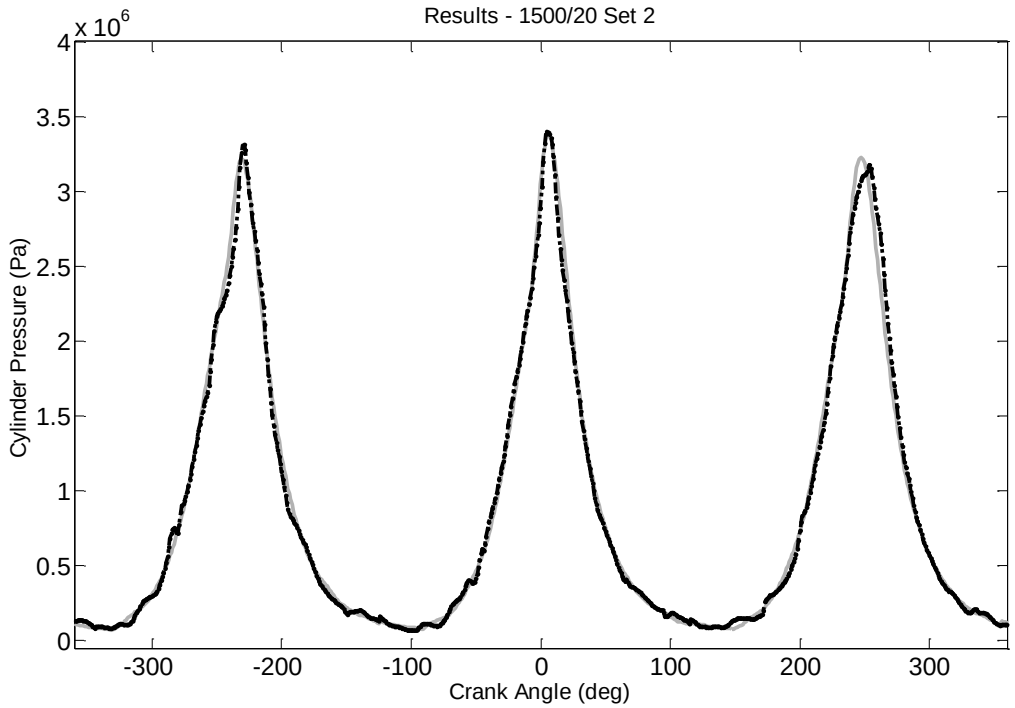

Figure 12. Condition-5 Block Vibration Generalisation Results –'moderate' case. Measured Cylinder Pressure (Grey Solid Line). Reconstructed Cylinder Pressure (Black Dashed Line). RMSE = 2.82%.

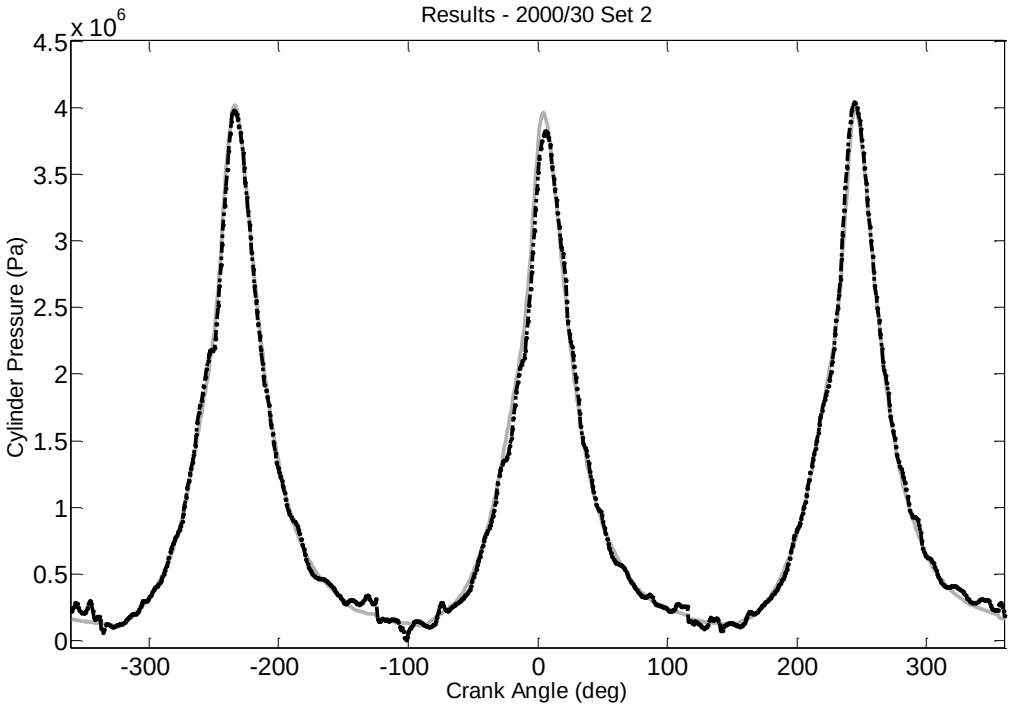

Figure 13. Condition-9 Block Vibration Generalisation Results –'moderate' case. Measured Cylinder Pressure (Grey Solid Line). Reconstructed Cylinder Pressure (Black Dashed Line). RMSE = 1.48%.